Experimental Study on Temperature Control Optimization of Ground Source Heat Pump Horizontal Headers

Xusong Tian [a], Ruiyong Mao [a*], Peng Pei [a], Hongwei Wu [c], Hong Ma [a], Cheng Hu [a], Zujing Zhang [a,b*]

[a] College of Civil Engineering, Guizhou University, Guiyang, 550025, China

[b] Guizhou Provincial Key Laboratory of Rock and Soil Mechanics and Engineering Safety, Guiyang, 550025, China

[c] School of Physics, Engineering and Computer Science, University of Hertfordshire, Hatfield, AL10 9AB, United Kingdom

E-mail addresses: rymao@gzu.edu.cn (R. Mao), zjzhang3@gzu.edu.cn (Z. Zhang).

Tel: +86 139 8505 6628 (R. Mao), +86 185 2391 9513 (Z. Zhang).

Abstract: The energy loss of ground source heat pump horizontal headers cannot be ignored. Based on the similarity theory and the principle of the orthogonal test, a sandbox experiment platform was built to study the temperature change rule of the horizontal header under the action of multiple factors and the influence of the temperature change on the U-tube heat exchange capacity. The results show that: (1) The influence degree of each factor on the horizontal header is as follows: buried depth > surface temperature > covering material > flow in the pipe; (2) Under the two extreme conditions, the temperature rise difference of the horizontal header water supply section is 0.25 ℃ and that of the return section is 0.29 ℃, the heat transfer difference of the water supply section is 91 W and that of the return section is 105 W and the heat exchange difference of the U-tube is 38.5 W; (3) The temperature rise in the return section of the horizontal header causes the loss of cold in the pipe, but the temperature rise in the water supply section promotes the heat exchange of the U-tube. Finally, the optimization methods and construction recommendations are put forward.

Key words: Ground source heat pump; Horizontal headers; Orthogonal test; Sandbox experiment; Heat exchange

1. Introduction

The State of the Global Climate 2020 [1] report released by the World Meteorological Organization listed four key climate change indicators: greenhouse gas concentration, sea-level rise, ocean heat and ocean acidification. These factors have a huge impact on the earth's ecological environment. Leveraging renewable energy is an excellent way to promote global sustainable development.

The heat pump [2] is an efficient energy-saving device that utilizes low-grade heat energy. Heat pumps include ground source heat pumps (GSHPs) [3,4], water source heat pumps [5,6] and air source heat pumps [7,8], which involve the transfer of heat and mass transfer [9]. It is worth mentioning that the ground source heat pump plays an important role in the utilization of shallow geothermal energy. In recent years, research on GSHPs has increased, covering many aspects, such as melting snow on pavement and bridges [10], heating greenhouses [11], proving cooling in tropical climates [12], etc. According to the literature, GSHPs have more economic advantages than the five conventional heating methods of electric resistance, fuel oil, liquid petrol gas, coal and oil when it is used for heating in winter [13]. During the cooling season, the average cooling coefficient of performance (COP) of the ground-coupled heat pump system for the horizontal ground heat exchanger (HGHE) in different trenches at 1 and 2 m depths is higher than that of the air-coupled heat pump system [14]. Due to its economic advantages, energy conservation and clean production, GSHP systems have become more and more widely used around the world.

Research on the performance of GSHPs has been a popular topic for a long time. Zhang et al. [15] studied the operation performance of the hybrid solar ground source heat pump (HSGSHP) system. The results show that solar space heating can improve the performance of the HSGSHP system by nearly 25.8%. Esen et al. conducted many studies on the performance prediction of GSHP systems. Based on experimental data, they predicted the COP of GSHP systems using an adaptive neuro-fuzzy inference system with different membership functions and fuzzy weighted pre-processing [16,17], artificial neural network [18] and support vector machines [19], respectively. Dong et al. [20] tested the thermal conductivity of different proportions of bone cement-based grouting. The results show that increasing the sand-cement ratio, maintaining high saturation, reducing porosity and adding high-performance aggregates are all ways to improve the thermal conductivity of materials, which can improve the heat transfer performance of vertical ground heat exchangers. Another way to improve the operational performance of ground source heat pumps is to reduce energy loss during the transmission process, which is rare in existing reports. Therefore, the focus of this study is to discuss the impact of different factors on the energy loss of horizontal headers and propose reasonable solutions.

There are two types of buried pipes used in GSHP systems: horizontal ground heat exchangers [21,22] and vertical ground heat exchangers [23,24]. Horizontal ground heat exchangers are divided into two series [25], parallel [26] and spiral [27]. The vertical ground heat exchanger is also divided: the pile foundation spiral buried pipe [28] and vertical U-shaped buried pipe [29]. HGHEs are easy to construct, but the heat exchange effect is poor. The vertical ground heat exchanger has a high heat exchange efficiency, but also a high initial investment. Therefore, selecting the appropriate buried pipe form can achieve a reasonable utilization of energy as well as reduce the cost of the investment. Through experiments, Liu et al. [30] analyzed the influence of the thermal deformation of the pipe and the gap width on the heat transfer of the horizontal buried pipe. Buried depth, solar radiation and the daily variation of sunshade will affect the heat transfer of HGHEs. Li et al. [31] studied the influence of surface boundary conditions, especially daytime shading, on the performance of the horizontal ground source heat pump system. The results show that different assumptions of surface boundary conditions have a significant impact on the results. The daily changes in solar radiation and shading will affect the outlet temperature of HGHEs until the buried depth is 2.5 m. It can be seen that the HGHE is greatly affected by surface factors. Similarly, because the horizontal header of the vertical ground heat exchanger is very shallow, surface factors have a large impact. Understanding the influence law can promote the development of the ground source heat pump, which is also the significance of this study.

The buried depth for vertical ground heat exchangers is usually around 100 m [32], which avoids the influence of surface factors. Therefore, the vertical ground heat exchanger is more widely used in ground source heat pump systems than the horizontal ground heat exchanger. Because the pile foundation spiral buried pipes are limited by the pile foundation, the vertical U-shaped buried pipe has higher applicability. This is also the reason why the vertical U-shaped buried pipe was selected as the underground heat exchanger in this study. The heat exchange of U-shaped vertical ground heat exchangers will be affected by many factors, including the inlet water temperature of the U-tube, water-containing cracks [33], the flow velocity in the U-tube and buried depth [34]. Researching how to improve the heat exchange of vertical U-tube heat exchangers is a constant difficulty. Wang et al. [35] demonstrated that soil with a high moisture content value has a strong heat dissipation capacity, which can improve the heat exchange of the U-tube. Pu et al. [36] showed that under laminar flow conditions, greater heat exchange can be obtained by increasing the Reynolds number and U-tube diameter. Chen et al. [37] introduced an enhanced U-tube borehole heat exchanger system, which connects one deviated deep hole with another vertical hole to form a closed loop that is stronger than the ordinary deep hole heat exchanger. Song et al. [38] established a vertical double U-shaped buried pipe heat transfer model and studied the influence of the thermal conductivity of borehole backfill material on the heat transfer of heat exchangers. The results show that in a certain range, increasing the thermal conductivity of borehole backfill material can improve the heat transfer of the U-tube. Because the temperature change of horizontal headers will affect the inlet temperature of the vertical ground heat exchangers, thereby affecting the heat exchange of the vertical ground heat exchangers, this study chose to analyze this problem.

The buried depth of horizontal headers is very shallow (generally 1.2 m) and is easily affected by various factors, resulting in the loss of cold and heat in the header. With the continuous expansion of the application and scale of the ground source heat pump [39], the pipe length, pipe diameter and flow rate of horizontal headers are also increasing. It can be seen that this part of energy loss cannot be ignored. At present, there are few studies on this aspect. The purpose of this study is to propose control measures against the energy loss of horizontal headers under the influence of multiple factors and improve the performance of the GSHP system. At the same time, it is to study the influence of the temperature change of horizontal headers on the heat transfer of vertical ground exchangers under the influence of multiple factors, put forward reference suggestions for actual GSHP projects and promote the development of the ground source heat pump.

Due to the high drilling cost and heavy workload, a sandbox test-bed is a common means for studying GSHP. Li et al. [40] conducted experimental and numerical studies on the transient heat transfer performance of ground heat exchangers (GHEs) in layered ground and built a 6.25 m × 1.5 m × 1 m test box. In order to extend the experimental results to practical projects, based on the similarity theory [41,42], Li et al. [43] built a test chamber filled with sand and clay to study the effect of heat load on the thermal performance of GHEs. Therefore, to reduce the experimental cost and extend the experimental results to practical projects, a 1.5 m × 1.5 m × 1.5 m experimental platform is built based on the similarity theory in this study.

When the experimental data results are affected by many factors, the orthogonal test [44,45,46] is a common experimental design method. Luo et al. [47] carried out orthogonal tests on the evaluation and optimization of the energy performance of deep borehole heat exchangers and obtained the order of the influencing factors. Su et al. [48] used the orthogonal test and variance analysis to study the effects of water velocity, pipe diameter and pipe inlet temperature on the heat transfer of GHEs. Li et al. [49] studied the heat transfer performance of buried pipes under the influence of multiple factors and levels through the orthogonal test and obtained the best combination of various factors on the best heat transfer performance of buried pipes and the contribution rate of various factors to the heat transfer performance of buried pipes. To explore the influence of multiple factors on horizontal headers, reduce the number of experimental groups, reduce experimental time and not affect the experimental results, the orthogonal test design is selected for the experiment.

In this study, the temperature change rule for the water supply and return sections of the horizontal header under the influence of multiple factors is explored. The changes in heat transfer of the horizontal header under different working conditions and their respective effects on the water supply and return sections of the horizontal header are analyzed. The difference between the heat transfer of the horizontal header under the most unfavourable and favourable condition is calculated. The innovation and significance are as follows: the influence of the temperature change of the horizontal header on the heat exchange of the vertical U-shaped buried heat exchanger is studied. The experimental data are processed by range analysis, and the most unfavourable factor affecting the temperature change of the horizontal header is obtained. The optimization methods of temperature control for the water supply and return sections of horizontal headers are summarized. Based on the experimental data, the construction recommendations for the actual ground source heat pump projects are proposed.

2. Experimental details

2.1. Experimental platform

The photos and schematic diagram of the experimental platform are shown in Figure 1. The experimental platform is composed of a sandbox, thermostatic water tank, data acquisition instrument, circulating water pump, rotameter, quartz heating tube and computer. The photos of these major pieces of equipment are shown in Figure 2, and the main technical parameters are shown in Table 1.

(a) Front of the experimental platform (b) Back of the experimental platform

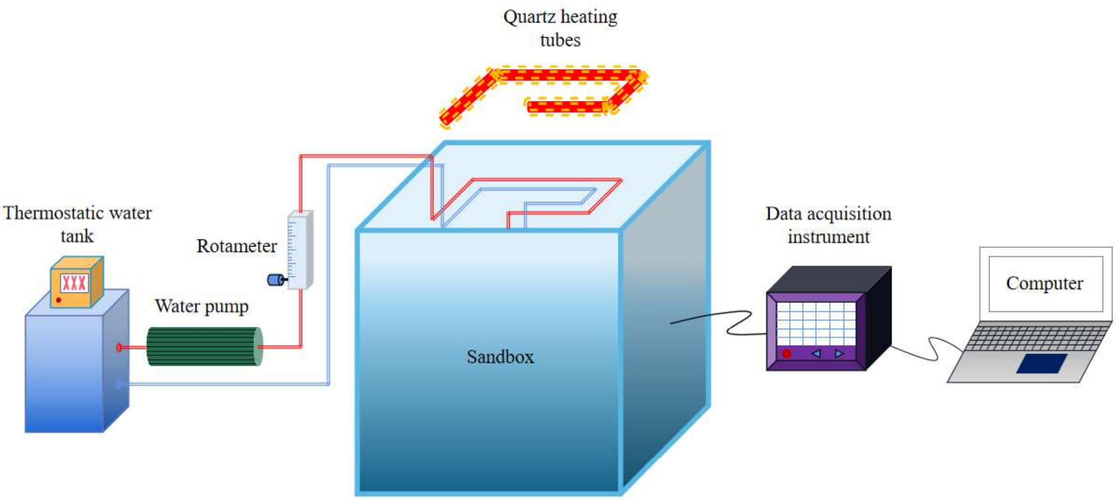

(c) Experimental schematic diagram

Fig. 1. Photos and schematic diagram of the experimental platform.

(a) Thermostatic water tank (b) Water circulating pump (c) Rotameter

(d) Data acquisition instrument (e) Quartz heating tube

Fig. 2. Photos of experimental equipment.

Table 1
Main technical equipment parameters.

Equipment	Technical Parameter	Remarks
Sandbox	1500 mm × 1500 mm × 1500 mm	Wrapped 30 mm insulation cotton
Thermostatic water tank	Temperature adjustment range: -5 ~ 100 ℃; Accuracy: 0.01 ℃	—
Water circulating pump	Power: 165 W; Lift: 28 m; Flow: 17 L/min	—
Rotameter	Flow regulation range: 0.6 ~ 6 L/min	—
Data acquisition instrument	36 channels; Recording interval 1 minute	—
Quartz heating tubes	Power: 800 W or 400 W	800 mm or 400 mm in length
Thermal resistance	Pt1000; Accuracy: 0.01 ± 0.005 ℃	3000 mm in length

The lower layer of the sandbox is equipped with dolomite at a thickness of 1.2 m. A 1 m long single U-tube heat exchanger is vertically buried in the centre of the sandbox, and the horizontal header is connected at the top of the U-tube. Due to the size limitation of the sandbox, the horizontal header is coiled to make its length reach about 2 m for both the water supply section and the return section. At the same time, the quartz heating tubes are arranged directly above the horizontal header following in the direction of the horizontal header.

2.2. Distribution of measuring points

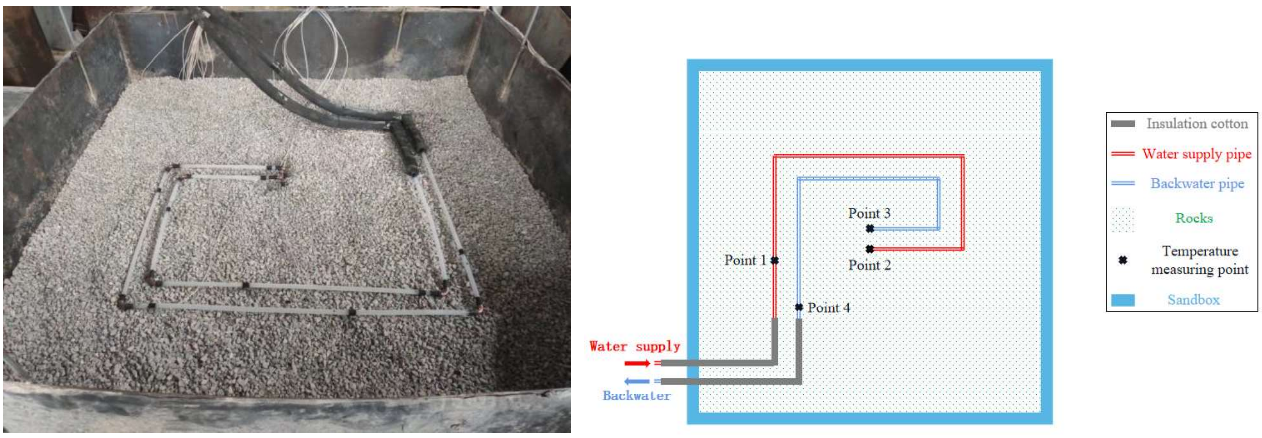

(a) Photo of the measuring points layout (b) Schematic diagram of the measuring points layout

Fig. 3. Layout of measuring points of the horizontal header.

Temperature measuring point 1 is arranged at the beginning of the water supply section of the horizontal header; temperature measuring point 2 is arranged at the water inlet of the U-tube; temperature measuring point 3 is arranged at the water outlet of the U-tube; and temperature measuring point 4 is arranged at the end of the return section of the horizontal header, as shown in Figure 3. Five temperature measuring points are arranged horizontally and eight are arranged vertically inside the sandbox to detect the influence range of temperature, as shown in Figure 4.

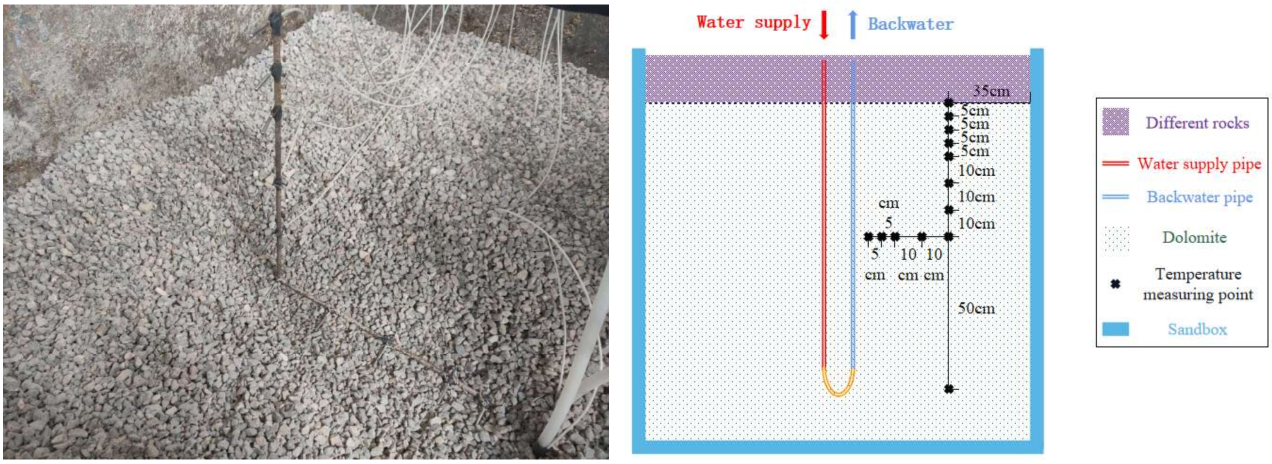

(a) Photo of the measuring points layout (b) Schematic diagram of the measuring points layout

Fig. 4. Layout of measuring points inside the sandbox.

2.3. Initial temperature field of the sandbox

The experiment was conducted in the spring, and the transverse and longitudinal initial temperature distribution in the sandbox is shown in Figure 5. It can be seen from Figure 5 (a) that the transverse temperature in the sandbox at the buried depth of 50 cm is unchanged before the experiment and remains at about 15.1 ℃. It can be inferred that at the same depth, the temperature in the horizontal direction is the same.

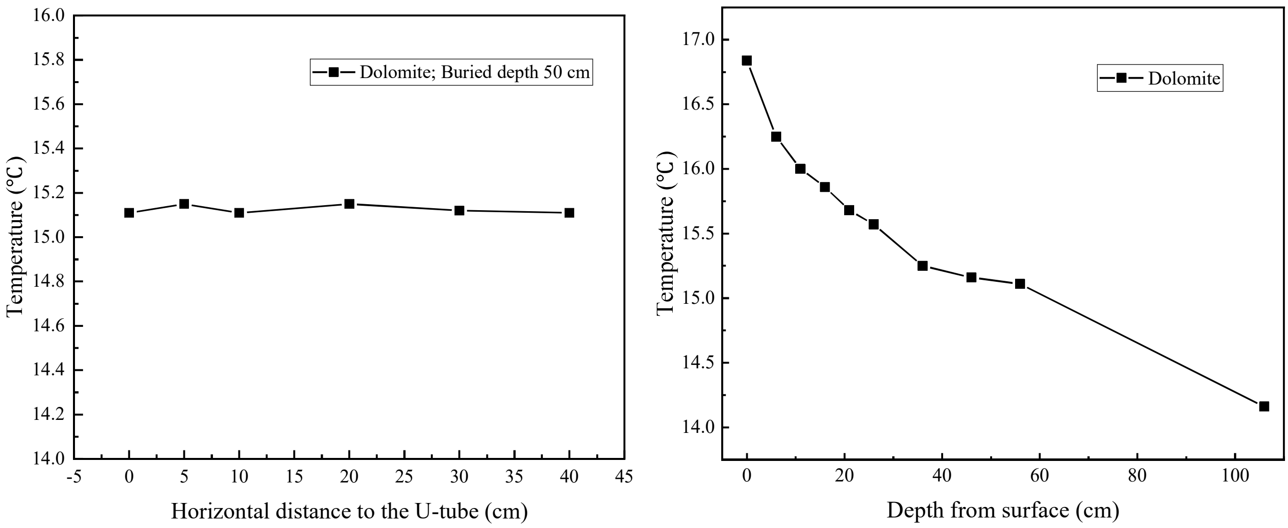

(a) Transverse (b) Longitudinal

Fig. 5. Initial soil temperature field.

It can be seen from Figure 5 (b) that the influence of external factors on the inside of the sandbox gradually decreases with the increase of depth, resulting in a constant decrease in temperature. When the depth is 106 cm, the temperature is 14.16 ℃, the surface temperature is 16.84 ℃ and the soil temperature in the middle is about 15 ℃.

2.4. Condition design

To extend the experimental conclusions to the actual ground source heat pump projects and improve the performance of the ground source heat pump system, the experimental platform is built based on the similarity theory. The similarity ratio is 40: 1. The main similarity design parameters are shown in Table 2.

Table 2
Similar design parameters.

Parameter type	Prototype	Similarity model	Similar multiple
Length of the horizontal header m	80	2	40: 1
Distance between the water supply section and return sections of the horizontal header cm	200	5	40: 1
Buried depth of the horizontal header cm	80 / 160 / 240	2 / 4 / 6	40: 1
Running time h	800	0.5	40^2: 1
Reynolds number	6362 / 8449 / 10536	6362 / 8449 / 10536	1: 1
Water temperature in the U-tube ℃	24	24	1: 1

Four common influencing factors, namely, the buried depth of the horizontal header, the flow in the pipe, the covering material and the surface temperature, were selected for the experiment to study the influence of the change of energy loss of the horizontal header and the change of temperature of the horizontal header on the heat exchange of the vertical U-tube under the combined action of multiple factors. To reduce the number of experimental groups, reduce the experimental time and not affect the experimental results, the L9 (3^4) orthogonal test table is selected, three different levels are selected for each factor and tests under 9 different working conditions are carried out, as shown in Table 3.

The buried depth is 2 cm, 4 cm and 6 cm, respectively; flow is 3 L/min, 4 L/min 5 L/min; the materials are dolomite, limestone and sandstone; and the surface temperature is set as 30 ℃, 35 ℃ and 40 ℃, respectively. At the same time, the initial working condition is designed as follows: the buried depth is 2 cm, the covering material is dolomite, the flow rate is 3L/min and the surface temperature is not treated and is the temperature of the day. The purpose is to compare the initial working condition with the data results of test No. 1 in Table 3, to obtain a rule and to extend this rule to other tests.

Table 3
Orthogonal test design.

Interfering factor / Test number	Buried depth of the header cm	Flow in pipe L/min	Covering material	Surface temperature ℃
1	2	3	Dolomite	30
2	4	5	Dolomite	35
3	6	4	Dolomite	40
4	2	5	Limestone	40
5	4	4	Limestone	30
6	6	3	Limestone	35
7	2	4	Sandstone	35
8	4	3	Sandstone	40
9	6	5	Sandstone	30

2.5. Experimental procedure

In the experiment, the main rocks used are dolomite, limestone and sandstone, with thermal a conductivity of 2.52 W/(m·K), 3.26 W/(m·K) and 2.78 W/(m·K), respectively. The flow is changed by the rotameter, the temperature of the rock surface covered by the horizontal header is changed by adjusting the hanging height of the quartz heating tube and the type and thickness of the rock covered are changed, as shown in Figure 6. To ensure the accuracy and validity of the temperature data results, the pipe section from the thermostatic water tank to the horizontal header is wrapped with insulation cotton at a thickness of 2 cm. After all the equipment is connected, commissioning is carried out and the

PT1000 thermal resistance is measured and corrected.

(a) 2 cm dolomite (b) 4 cm limestone (c) 6 cm sandstone

Fig. 6. Rocks of different types and thicknesses.

Taking the experiment of working condition 1 as an example, the experimental steps are as follows:

(1) Set the recording interval of the data acquisition instrument to 1 minute each time;

(2) Cover the horizontal header with 2 cm of dolomite;

(3) Hang the quartz heating tubes on the iron frame above the sandbox with iron wire. Place a PT1000 thermal resistor directly below each quartz heating pipe, that is, on the surface of the dolomite, to measure the rock surface temperature.

(4) Adjust the rock surface temperature to about 30 ℃ by adjusting the hanging height of the heating pipe and the start and stop of the switch;

(5) Set the temperature of the thermostatic water tank to 24 ℃, so that the inlet temperature of the horizontal header is 24 ℃;

(6) Open the circulating water pump and adjust the knob of the rotameter to control the flow at 3 L/min;

(7) Shut down the system after 30 minutes of operation;

(8) Collect the temperature data from the data acquisition instrument and use the computer for analysis and processing.

The experimental procedure under other working conditions is similar to that under working condition 1. The test time of each group is 0.5 hours. After the test of each working condition is completed, to restore the rock temperature field in the sandbox without affecting the next test, the next group of tests can be carried out after an interval of 24 hours.

3. Results

3.1. Analysis on temperature change of the horizontal header under the initial working condition

The initial working condition is: the buried depth is 2 cm, the covering material is dolomite, the flow rate is 3 L/min, and the surface temperature is 16.59 ℃ (the temperature of that day). After running the system for 0.5 hours, the temperature change of each measuring point is as shown in Figure 7.

It can be seen from Figure 7 that after running the experiment for 6 minutes, the temperature of each measuring point gradually tends to balance. At 0.5 hours, the temperature does not change. At this time, point 1, point 2, point 3 and point 4 respectively rise from 16.55 °C, 16.55 °C, 16.56 °C and 16.55 °C to 22.71 °C, 22.67 °C, 22.64 °C and 22.61 °C. After reaching a steady state, the temperature decreases from point 1 to point 2 (the horizontal header water supply section), point 2 to point 3 (the vertical U-tube section) and point 3 to point 4 (the horizontal header water return section), by 0.04 °C, 0.03 °C and 0.03 °C, respectively. This is because the inlet water temperature is set at 24 °C, while the lower air temperature and soil temperature remove the heat in the pipe.

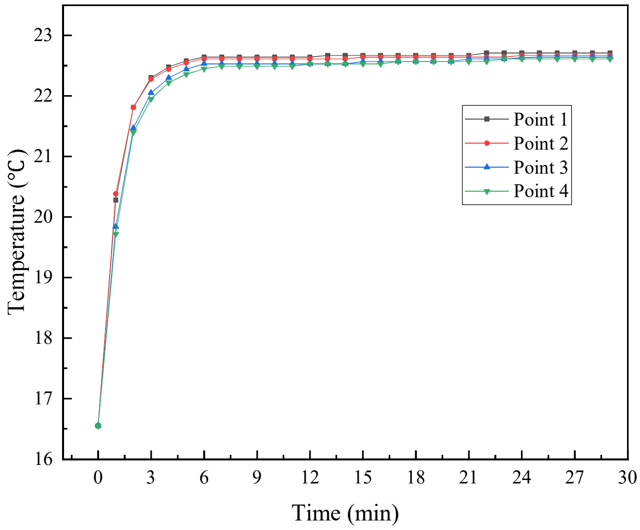

Fig. 7. Temperature change of measuring points of the horizontal header under the initial working condition.

3.2. Analysis of temperature change of the horizontal header under orthogonal test conditions

3.2.1. Temperature changes when the buried depth is 2 cm

The horizontal header is covered with dolomite, limestone and sandstone at a thickness of 2 cm, respectively. At the same time, the rock surface temperature and flow in the pipe are controlled and tests No. 1, No. 4 and No. 7 as shown in Table 3 are carried out. The temperature changes of each measuring point within 0.5 h are shown in Figure 8.

As shown in Figure 8 (a), the temperature at each measuring point is unchanged after 0.5 h. At points 1, 2, 3 and 4, the temperature rises from 16.99 °C, 16.98 °C, 16.99 °C and 16.99 °C to 23.11 °C, 23.29 °C, 23.16 °C and 23.37 °C, respectively. The temperature rises sharply in the first 6 minutes, then gradually flattens and finally reaches basic stability. At this time, the temperature from point 1 to point 2 rises by 0.18 °C, the temperature from point 2 to point 3 drops by 0.13 °C and the temperature from point 3 to point 4 rises by 0.21 °C.

Due to the shallow buried depth, the horizontal header is affected by the surface temperature of the covered rock. The temperature of the water supply and return sections rises from the beginning to the end. From the inlet to the outlet of the U-tube, the fluid in the pipe exchanges heat with the surrounding low-temperature rocks and the temperature is reduced, with a reduction of 0.13 °C.

Compared with the initial working condition, the parameter design of test No. 1 is only different in the surface temperature. It can be seen from the comparison that after 0.5 h, due to the influence of the surface temperature, the temperature of the water supply and return sections of the horizontal header increased under the test No. 1 working condition, while the initial working condition showed the opposite trend. At the same time, due to the influence of the surface temperature, the inlet water temperature of the U-tube of test No. 1 is higher than the initial working condition, the temperature difference between the U-tube and the surrounding soil is increased and the heat exchange effect is improved. The temperature difference between the inlet and outlet of the U-tube in test 1 is 0.13 °C, which is 0.10 °C higher than the 0.03 °C under the initial working condition. It can be speculated that under other orthogonal test conditions, if only the surface temperature is changed, the same result can be obtained and increasing the inlet water temperature of the U-tube can promote heat exchange and increase the temperature difference between the inlet and outlet of the U-tube.

As shown in Figure 8 (b), within 0.5 hours, it is found that the temperature at each measuring point rises continuously and cannot reach a stable state. At 0.5 hours, point 1, point 2, point 3 and point 4 increased from the initial 16.63 °C, 16.65 °C, 16.64 °C and 16.63 °C to 23.95 °C, 24.27 °C, 24.13 °C and 24.50 °C, respectively. The temperature rose sharply in the first 3 minutes and then levelled off, but it still maintained a rapid growth within 0.5 hours. At 0.5 hours, point 1 to point 2 increased by 0.32 °C, point 2 to point 3 decreased by 0.14 °C, and point 3 to point 4 increased by 0.37 °C.

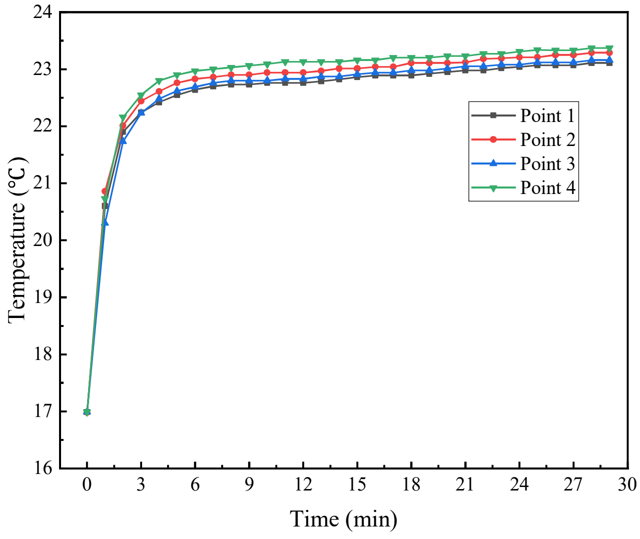

(a) Test No. 1: 2 cm; 3 L/min; Dolomite; 30 °C

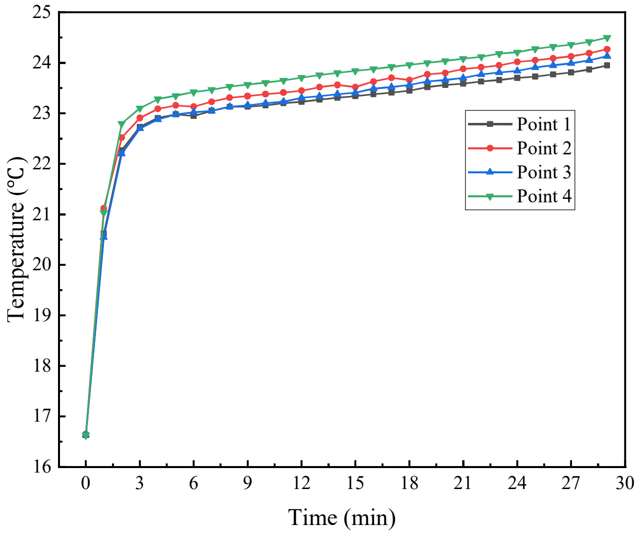

(b) Test No. 4: 2 cm; 5 L/min; Limestone; 40 °C

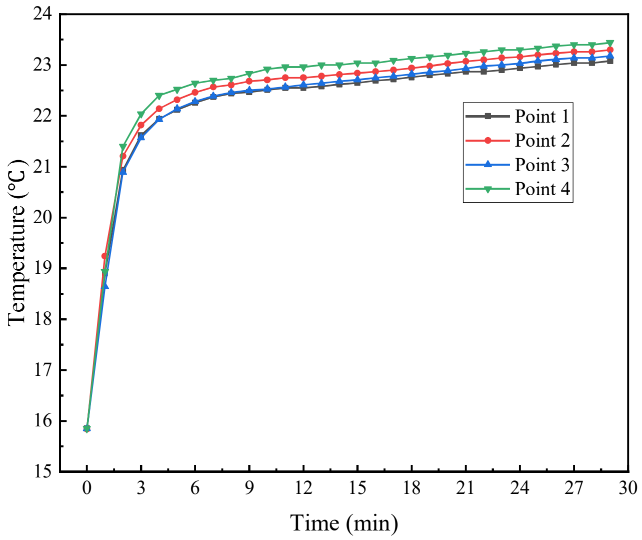

(c) Test No. 7: 2 cm; 4 L/min; Sandstone; 35 °C

Fig. 8. Temperature changes at the measuring points of the horizontal header with the buried depth of 2 cm.

Compared with test No. 1, it can be found that under the premise of the same buried depth, the temperature increase of both the water supply section and the return section changed greatly due to the surface temperature of the covered rock being 40 °C and the maximum thermal conductivity of limestone. At the same time, due to the increased flow rate and inlet water temperature in the U-tube, the temperature difference between the U-tube and the surrounding rocks is greater, and the heat exchange is more obvious, resulting in the difference between the inlet and outlet water temperature of the U-tube finally reaching 0.14 °C.

As shown in Figure 8 (c), within 0.5 hours, the temperature change trend of each measuring point is similar to test No. 4. At 0.5 h, the temperatures of point 1, point 2, point 3 and point 4 increased from the initial 15.85 °C, 15.84 °C, 15.85 °C and 15.85 °C to 23.08 °C, 23.30 °C, 23.18 °C and 23.44 °C, respectively. The temperature rose sharply in the first 4 minutes and then maintained rapid growth. At 0.5 hours, point 1 to point 2 increased by 0.22 °C, point 2 to point 3 decreased by 0.12 °C and point 3 to point 4 increased by 0.26 °C.

Compared with test No. 4, it can be found that since the thermal conductivity of sandstone is second only to that of limestone, the buried depth is the same and the surface temperature of the covered rock only reaches 35 °C, the temperature increase values from point 1 to point 2 and from point 3 to point 4 are lower than those of test No. 4. As for the inlet temperature and flow in the U-tube, test No. 7 was lower than test No. 4, resulting in poor heat exchange between the U-tube and the surrounding rocks. Finally, the temperature difference at the inlet and outlet of the U-tube was 0.02 °C lower than that of test No. 4.

3.2.2. Temperature changes when the buried depth is 4 cm

The horizontal header is covered with dolomite, limestone and sandstone at a thickness of 4 cm, respectively. At the same time, the rock surface temperature and flow in the pipe are controlled, and tests No. 2, No. 5 and No. 8 as shown in Table 3 are conducted. Within 0.5 h, the temperature change of each measuring point is shown in Figure 9.

As shown in Figure 9 (a), the temperature at each measuring point is unchanged after 0.5 h. At points 1, 2, 3 and 4, the temperature rises from 16.73 °C, 16.74 °C, 16.75 °C and 16.74 °C to 23.04 °C, 23.18 °C, 23.13 °C and 23.28 °C, respectively. The temperature rises sharply in the first 8 minutes, then gradually flattens and finally reaches basic stability. At this time, the temperature rises by 0.14 °C from point 1 to point 2, decreases by 0.05 °C from point 2 to point 3, and increases by 0.15 °C from point 3 to point 4.

Compared with test No. 1, it can be found that the increase of the thickness of the covering material inhibits the heat exchange between the horizontal header and the surface temperature of the covered rock, which reduces the temperature increase of the water supply and return sections of the horizontal header. From the inlet to the outlet of the U-tube, the fluid in the pipe exchanges heat with the surrounding low-temperature rocks, reducing the temperature. However, due to the decrease of the inlet temperature and the increase of the flow in the pipe, the temperature reduction value is smaller than that of test No. 1.

As shown in Figure 9 (b), the temperature change trend of each measuring point is similar to test No. 2. The temperatures of points 1, 2, 3 and 4 increase from 16.49 °C, 16.50 °C, 16.49 °C and 16.49 °C to 23.04 °C, 23.21 °C, 23.14 °C and 23.31 °C, respectively. The temperature rises sharply in the first 6 minutes and then gradually reaches stability. At this time, the temperature from point 1 to point 2 rises by 0.17 °C, the temperature from point 2 to point 3 drops by 0.07 °C and the temperature from point 3 to point 4 rises by 0.17 °C.

Compared with test No. 2, the coverage thickness of 4 cm is the same. Although the surface temperature of the covered rock in test No. 2 is 5 °C higher than that of test No. 5, the temperature increase of the water supply and return sections of the horizontal header is higher than that of test No. 2 because the thermal conductivity of limestone is greater than that of dolomite. At the same time, as for the inlet temperature of the U-tube, the temperature value of test No. 5 is also higher than that of test No. 2. Because the flow of the two tests is different, the inlet and outlet temperature difference are finally maintained at 0.07 °C. By conducting a comparison with test No. 4, it can be found that due to the increase of buried depth and the decrease of the surface temperature of the covered rock, the temperature change curves of point 1, point 2, point 3 and point 4 also have great changes compared with test No. 4, and the temperature of the four test points at 0.5 h is lower than that of test No. 4.

As shown in Figure 9 (c), the temperature at each measuring point cannot reach a stable state within 0.5 h, which is similar to test No. 7. At 0.5 hours, the temperatures of points 1, 2, 3 and 4 increased from the initial 16.56 °C, 16.56 °C, 16.57 °C and 16.56 °C to 23.00 °C, 23.24 °C, 23.12 °C and 23.35 °C, respectively. The temperature rose sharply in the first 4 minutes, and then maintained rapid growth. At 0.5 hours, point 1 to point 2 increased by 0.24 °C, point 2 to point 3 decreased by 0.12 ℃ and point 3 to point 4 increased by 0.23 ℃.

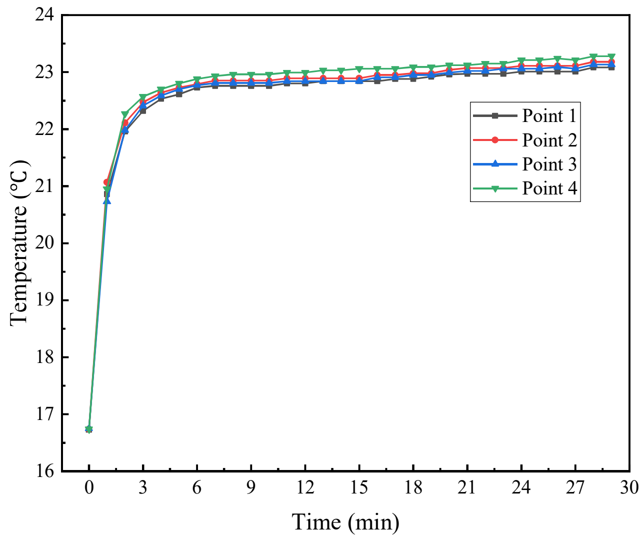

(a) Test No. 2: 4 cm; 5 L/min; Dolomite; 35 ℃

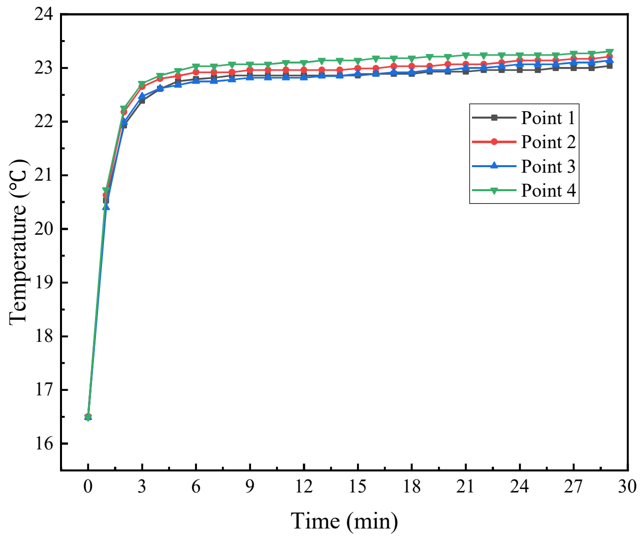

(b) Test No. 5: 4 cm; 4 L/min; Limestone; 30 ℃

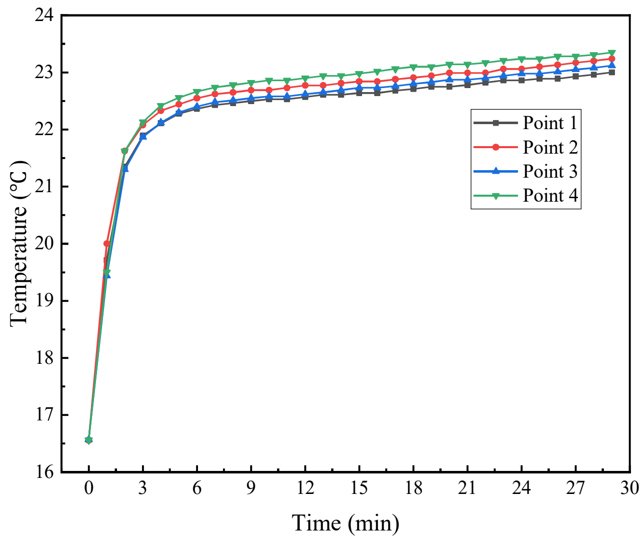

(c) Test No. 8: 4 cm; 3 L/min; Sandstone; 40 ℃

Fig. 9. Temperature changes at the measuring points of the horizontal header with the buried depth of 4 cm.

Compared with test No. 7, it can be found that due to the increase in the surface temperature of the covered rock and the relatively large thermal conductivity of sandstone, the increase of 2 cm based on the buried depth of test No. 7 does not significantly inhibit the temperature rise at each measuring point, resulting in the temperature value increases from point 2 to point 3 and from point 3 to point 4 to be close to that of test No. 7. At the same time, the inlet and outlet temperature difference of the U-tube is also the same as that of test No. 7.

3.2.3. Temperature changes when the buried depth is 6 cm

The horizontal header is covered with dolomite, limestone and sandstone at a thickness of 6 cm, respectively. At the same time, the rock surface temperature and flow in the pipe are controlled, and tests No. 3, No. 6 and No. 9 as shown in Table 3 are conducted. The temperature change of each measuring point within 0.5 h, is shown in Figure 10.

As shown in Figure 10 (a), the temperature at each measuring point is unchanged after 0.5 h. The temperatures of point 1, point 2, point 3 and point 4 increased from 16.82 ℃, 16.82 ℃, 16.82 ℃ and 16.81 ℃ to 23.08 ℃, 23.18 ℃, 23.13 ℃ and 23.24 ℃, respectively. The temperature increased sharply in the first 6 minutes, then gradually levelled off and finally reached basic stability. At this time, the temperature from point 1 to point 2 increased by 0.10 ℃, from point 2 to point 3 decreased by 0.05 ℃ and from point 3 to point 4 increased by 0.11 ℃.

Compared with test No. 2, it can be found that as the buried depth is once again increased, although the surface temperature of the covered rock rises to 40 ℃, the heat exchange between the horizontal header and the surface temperature of the covered rock is not obvious, and the temperature rise values from point 1 to point 2 and from point 3 to point 4 are lower than that of test No. 2. From the inlet to the outlet of the U-tube, the temperature reduction value is the same as that of test No. 2 due to the influence of the flow change.

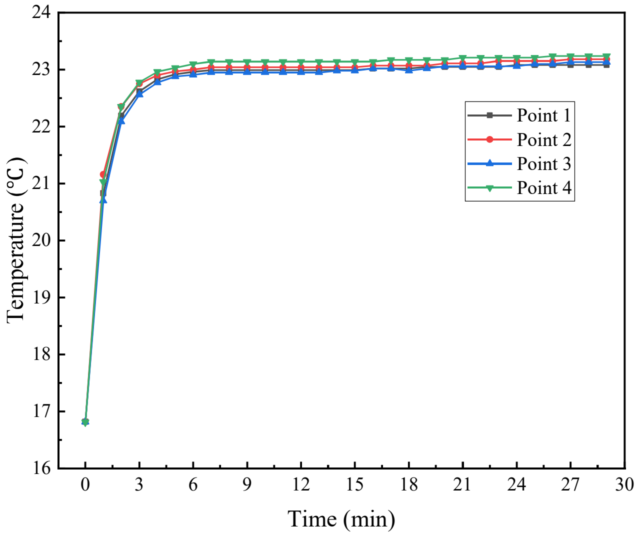

(a) Test No. 3: 6 cm; 4 L/min; Dolomite; 40 ℃

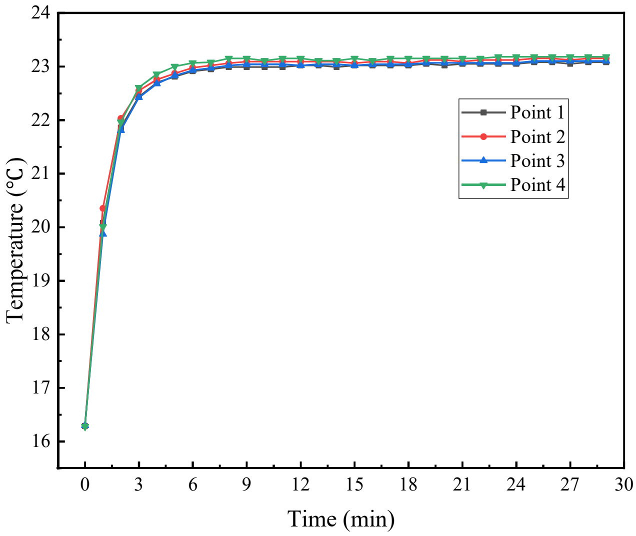

(b) Test No. 6: 6 cm; 3 L/min; Limestone; 35 ℃

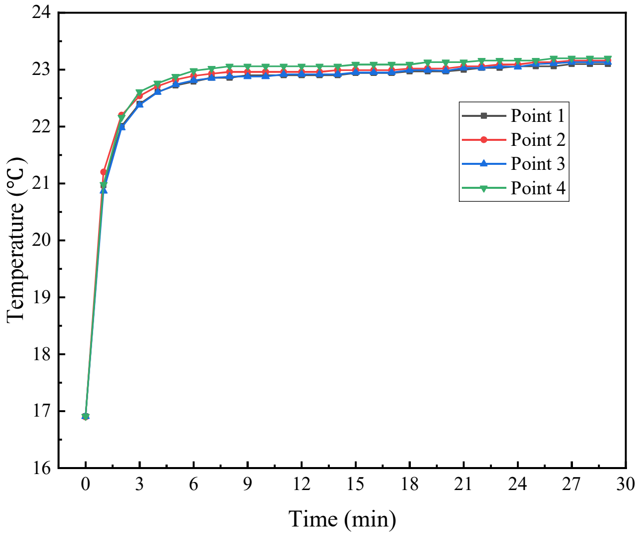

(c) Test No. 9: 6 cm; 5 L/min; Sandstone; 30 ℃

Fig. 10. Temperature changes at the measuring points of the horizontal header with the buried depth of 6 cm.

As shown in Figure 10 (b), within 0.5 hours, the temperature change trend of each measuring point is similar to test No. 3. At points 1, 2, 3 and 4, the temperature rises from 16.29 ℃, 16.29 ℃, 16.30 ℃ and 16.28 ℃ to 23.08 ℃, 23.15 ℃, 23.10 ℃ and 23.18 ℃, respectively. The temperature rises sharply in the first 7 minutes, then gradually flattens, and finally reaches a stable state. At this time, the temperature from point 1 to point 2 rises by 0.07 ℃, from point 2 to point 3 drops by 0.05 ℃ and from point 3 to point 4 rises by 0.08 ℃.

Compared with test No. 5, it can be found that, without changing the type of covered rock, the buried depth increases again. Although the surface temperature of the covered rock increases by 5 ℃, it does not have much impact on the heat exchange between the horizontal header and the covered rock, and the temperature increase values from point 1 to point 2 and from point 3 to point 4 are also lower than that of test No. 5. Because the water temperature at the inlet of the U-tube is lower than that of test No. 5, and the temperature difference with the rock in the sandbox is smaller, it results in no obvious heat exchange, and the temperature difference between the inlet and outlet is only 0.05 °C, which is 0.02 °C lower than that of test No. 5.

As shown in Figure 10 (c), after 0.5 hours, the temperature at each measuring point is unchanged. At points 1, 2, 3 and 4, the temperature rises from 16.91 °C, 16.90 °C, 16.91 °C and 16.91 °C to 23.10 °C, 23.16 °C, 23.13 °C and 23.20 °C, respectively. The temperature rises sharply in the first 6 minutes, then gradually flattens and finally reaches basic stability. At this time, the temperature rises by 0.06 °C from point 1 to point 2, decreases by 0.03 °C from point 2 to point 3 and increases by 0.07 °C from point 3 to point 4.

Compared with test No. 8, it can be found that due to the increase of the buried depth and the decrease of the surface temperature of the covered rock, the temperature of the fluid in the horizontal header is basically not affected by the external environment, and the temperature rise values from point 1 to point 2 and point 3 to point 4 are greatly reduced. Therefore, the inlet temperature of the U-tube is reduced, the temperature difference with the rock in the sandbox is reduced and the heat exchange is not obvious. Because of this, naturally, the temperature difference between the inlet and outlet will decrease.

In summary, test No. 4 is the most unfavourable working condition, as it has a large impact on the temperature of the horizontal header, resulting in a temperature increase of the water supply and return sections of 0.32 °C and 0.37 °C, respectively. Although the temperature of the return section cannot be kept constant, it can increase the temperature difference between the U-tube and the surrounding rock and soil, promote the heat exchange of the vertical U-tube, increase the temperature difference between the inlet and the outlet of the U-tube and make the temperature difference between the inlet and the outlet reach 0.14 °C. Test No. 9 is the most favourable working condition, as it has little impact on the horizontal header, resulting in a temperature increase of the water supply and return sections of 0.06 °C and 0.07 °C, respectively, and the temperature of the return section remains relatively constant. However, due to the small temperature increase of the water supply section, it is not conducive to the heat exchange of the U-tube, and the temperature difference between the inlet and the outlet of the U-tube is only 0.03 °C.

3.3. Heat transfer of the water supply and return sections of the horizontal header

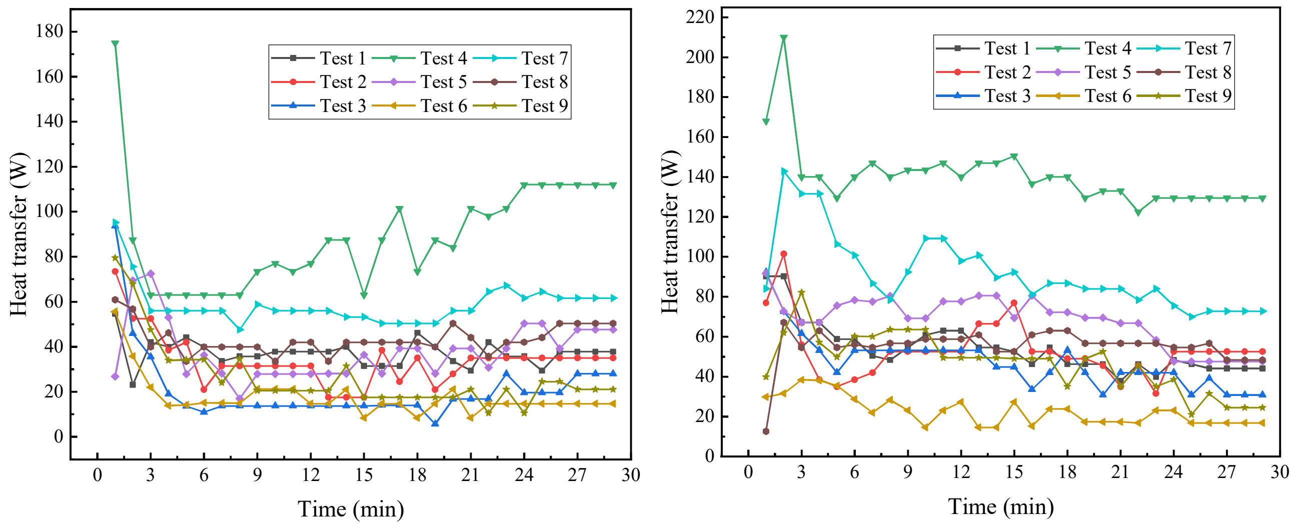

(a) Heat transfer in the supply section (b) Heat transfer in the return section

Fig. 11. Heat transfer of the water supply section and return sections of the horizontal header.

As shown in Figure 11, the heat transfer [50] of the water supply section of the horizontal header is different under different working conditions, and the heat transfer of the return section is also different. As the laying methods and lengths of the water supply and return sections of the horizontal header are the same, the heat transfer of the water supply and return sections under the same working conditions are similar. At first, the heat transfer change in the water supply and return sections of the horizontal header was complex and irregular, but test No. 4 remained at a high state. Finally, the heat transfer under various working conditions gradually stabilized. When stable, the heat transfer of the water supply section of the horizontal header from test No. 1 to No. 9 is 37.8 W, 35.0 W, 28.0 W, 112.0 W, 47.6 W, 14.7 W, 61.6 W, 50.4 W and 21.0 W, respectively. The heat transfer of the return section is 44.1 W, 52.5 W, 30.8 W, 129.5 W, 47.6 W, 16.8 W, 72.8 W, 48.3 W and 24.5 W, respectively.

The heat transfer of the water supply and return sections is the highest in test No. 4 (the most unfavourable working condition), which is 112.0 W and 129.5 W, respectively. At this time, the temperature increase of the water supply and return sections is 0.32 ℃ and 0.37 ℃, respectively, which is also the highest of the 9 tests conducted. This is due to the large thermal conductivity of limestone, the shallow buried depth, high surface temperature, large flow in the pipe and large impact on the horizontal header.

The heat transfer of the water supply and return sections is the lowest in test No. 6, which is 14.7 W and 16.8 W, respectively. At this time, the temperature increase of the water supply and return sections is 0.07 ℃ and 0.08 ℃, respectively. The heat transfer of the water supply and return sections of test No. 9 (the most favourable working condition) is 21.0 W and 24.5 W, respectively, and the temperature rise of the water supply and return sections is 0.06 ℃ and 0.07 ℃, respectively. It is found that the temperature rise of the water supply and return sections of test No. 9 is lower than that of test No. 6, but the heat transfer of the water supply and return sections of test No. 9 is higher than that of test No. 6 due to the larger flow of test No. 9.

3.4. Effect of the horizontal header on U-tube heat exchange

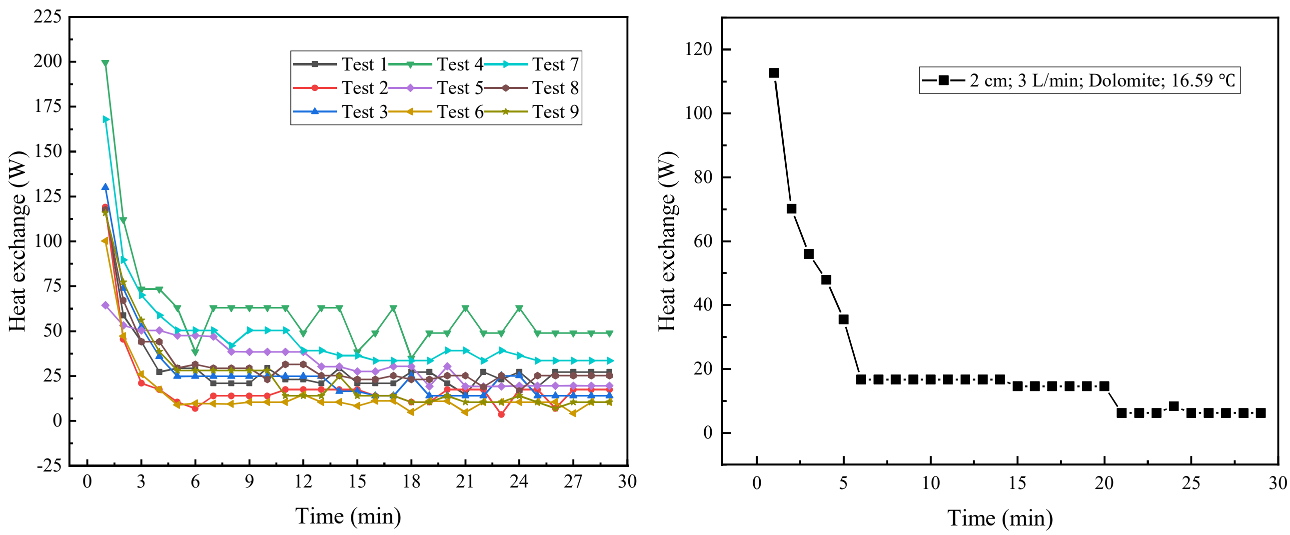

(a) Heat exchange curves of tests No. 1 to No. 9 (b) Heat exchange curve under initial working condition

Fig. 12. The heat exchange of the U-tube.

Under the effect of different temperature increases in the water supply section of the horizontal header, the heat exchange change [51] of the U-tube under different working conditions is shown in Figure 12. It can be seen from the figure that the heat exchange rate is at the maximum at the beginning, then gradually decreases, and finally tends to be stable. When the heat exchange reaches stability, the heat exchange of the U-tube in tests No. 1 to No. 9 is 27.30 W, 17.50 W, 14.00 W, 49.00 W, 19.60 W, 10.50 W, 33.60 W, 25.20 W and 10.50 W, respectively, and the heat exchange under the initial condition is 6.30 W. Under the influence of multiple factors, the heat exchange of test No. 4 is the largest, while that of test No. 6 and test No. 9 is the smallest and the same. However, the heat exchange of the U-tube under all orthogonal test conditions is higher than the initial condition. It can be seen that under the orthogonal test conditions, the

U-tube is affected more than the initial condition, and when the buried depth is shallow, the thermal conductivity of the overburden rock is large, the surface temperature is high and the flow rate in the pipe is large, the impact on the U-tube is greatest; otherwise, the impact is minimal.

Table 4

Comparison of heat exchange of the U-tube under different working conditions.

Test number	1	6	8	3	5	7	2	4	9
Flow rate L/min	3	3	3	4	4	4	5	5	5
U-tube inlet temperature ℃	23.29	23.15	23.24	23.18	23.21	23.30	23.18	24.27	23.16
U-tube outlet temperature ℃	23.16	23.10	23.12	23.13	23.14	23.18	23.13	24.13	23.13
Temperature difference between the U-tube inlet and outlet ℃	0.13	0.05	0.12	0.05	0.07	0.12	0.05	0.14	0.03
U-tube heat exchange W	27.30	10.50	25.20	14.00	19.60	33.60	17.50	49.00	10.50

As the heat exchange is related to the flow rate, by looking at Table 4 when the flow rate is 3 L/min and the flow rate is unchanged, it can be found by comparing tests No. 1, No. 6 and No. 8 that the inlet temperature of the U-tube is 23.29 ℃, 23.15 ℃ and 23.24 ℃, respectively, and the heat exchange of the U-tube is 27.30 W, 10.50 W and 25.20 W, respectively. When the flow rate is 4 L/min, it can be found by comparing tests No. 3, No. 5 and No. 7 that the inlet temperature of the U-tube is 23.18 ℃, 23.21 ℃ and 23.30 ℃, respectively, and the heat exchange of the U-tube is 14.00 W, 19.60 W and 33.60 W, respectively. When the flow rate is 5 L/min, it can be found by comparing tests No. 2, No. 4 and No. 9 that the inlet temperature of the U-tube is 23.18 ℃, 24.27 ℃ and 23.16 ℃, respectively, and the heat exchange of the U-tube is 17.50 W, 49.00 W and 10.50 W, respectively. It can be seen that when the flow rate is constant, increasing the water temperature at the inlet of the U-tube can strengthen the heat exchange between the U-tube and the surrounding rocks and increase the heat exchange, which proves the conjecture in Section 3.2.1.

However, blindly increasing the inlet water temperature of the U-tube will also increase the outlet temperature of the U-tube, which does not comply with the requirements of the unit. Therefore, when the requirements of unit temperature and flow are met, the heat exchange can be improved by increasing the end temperature of the water supply section of the horizontal header.

3.5. The temperature rise of the water return section of the horizontal header is affected by various factors

3.5.1. The temperature rise value of the water return section

From the above analysis, it can be seen that under various experimental conditions, the temperature rise will occur from the beginning to the end of the water supply and return sections of the horizontal header, and various factors have similar effects on the water supply and return sections. However, within a certain range, the temperature rise of the water supply section will increase the inlet water temperature of the U-tube and improve the heat exchange effect. In contrast, the temperature rise in the return section of the horizontal header is not conducive to keeping the temperature constant in the return section of the horizontal header, which is an undesired result. Therefore, the return section of the horizontal header is studied here for temperature rise analysis.

Table 5

The temperature rise of the water return section of the horizontal header.

Test number	1	2	3	4	5	6	7	8	9
Point 3 Temperature ℃	23.16	23.13	23.13	24.13	23.14	23.10	23.18	23.12	23.13
Point 4 Temperature ℃	23.37	23.28	23.24	24.50	23.31	23.18	23.44	23.35	23.20
Temperature rise ℃	0.21	0.15	0.11	0.37	0.17	0.08	0.26	0.23	0.07

After 0.5 hours, the temperatures at point 3 and point 4 are stable. The temperatures of point 3 and point 4 and the temperature rise value from point 3 to point 4 are shown in Table 5. It can be seen from the table that the maximum

temperature rise in the water return section occurs in test No. 4 and the minimum occurs in test No. 9. It can be inferred that the parameter settings of test No. 4 have the greatest impact on the horizontal header. In contrast, under the parameter settings of test No. 9, the influence is minimal.

3.5.2. Temperature rise range analysis

Table 6 shows the range analysis [52] on the temperature rise of the horizontal header return section obtained from the orthogonal test, where K_1 is the sum of the temperature rise values in the return section corresponding to the first level of each factor, K_2 is the sum of the temperature rise values in the water return section corresponding to the second level of each factor, and K_3 is the sum of the temperature rise values in the water return section corresponding to the third level of each factor.

Table 6

Range analysis of the orthogonal test.

Interfering factor / Test number	Buried depth of the header cm	Flow in the pipe L/min	Covering material	Surface temperature ℃	Return water temperature rise ℃
1	2	3	Dolomite	30	0.21
2	4	5	Dolomite	35	0.15
3	6	4	Dolomite	40	0.11
4	2	5	Limestone	40	0.37
5	4	4	Limestone	30	0.17
6	6	3	Limestone	35	0.08
7	2	4	Sandstone	35	0.26
8	4	3	Sandstone	40	0.23
9	6	5	Sandstone	30	0.07
K_1	0.84	0.52	0.47	0.45	
K_2	0.55	0.54	0.62	0.49	
K_3	0.26	0.59	0.56	0.71	
$\kappa_1\left(=\frac{K_1}{3}\right)$	0.280	0.173	0.157	0.150	
$\kappa_2\left(=\frac{K_2}{3}\right)$	0.183	0.180	0.207	0.163	
$\kappa_3\left(=\frac{K_3}{3}\right)$	0.087	0.197	0.187	0.237	
Range	0.193	0.023	0.050	0.087	
Poor scheme	2	5	Limestone	40	
Excellent scheme	6	3	Dolomite	30	

It can be seen from Table 6 that the influence of buried depth, flow in the pipe, covering material and surface temperature on the heat transfer of the return section of the horizontal header is in the following order: buried depth > surface temperature > covering material > flow in the pipe. At the same time, the poor scheme is test No. 4, and the excellent scheme is 6 cm; 3 L/min; dolomite; 30 ℃. This scheme does not appear among the 9 tests in Table 3. The closest one to this scheme is test No. 9. It can be seen from Table 5 that the temperature rise of test No. 9 is indeed the lowest, which is consistent with the above speculation. In addition, in the optimal scheme parameter settings, the thickness of the covered rock is the largest, the flow in the pipe is the smallest, the thermal conductivity of the covered rock is the smallest and the surface temperature of the covered rock is the lowest, which isolates the influence of external factors on the water return section of the horizontal header to the greatest extent. It can be determined that this scheme is the best one.

To prove the above results again, the heat transfer of the water supply section of the horizontal header is taken here for a similar range analysis, and the range of the buried depth of the header, the flow in the pipe, the covering materials, and the surface temperature are 49.233, 21.700, 24.500 and 28.000, respectively. It can be seen that the order of influence of the four factors on the heat transfer of the backwater section of the horizontal header is still: buried depth > surface temperature > covering material > flow in the pipe. At the same time, the same conclusion can also be drawn from the range analysis that the poor scheme is test No. 4, and the excellent scheme is 6 cm; 3 L/min; dolomite; 30 ℃.

4 Discussion

4.1. Optimization methods for temperature control of the horizontal header

It can be seen from the analysis in Section 3 that the influence degree of the four factors of buried depth, flow in the pipe, covering material and surface temperature on the horizontal header is as follows: buried depth > surface temperature > covering material > flow in the pipe. When the buried depth is shallow, the thermal conductivity of the covering material is high, the surface temperature is high, the flow rate in the pipe is high, the temperature change of the horizontal header is obvious, and the heat transfer is the largest. In contrast, the temperature rise and the heat gain are small. The temperature rise of the water supply section of the horizontal header can increase the temperature difference between the vertical ground heat exchangers and the surrounding rocks and improve the heat exchange. However, the temperature rise of the water return section is not conducive to the preservation of the internal cold quantity of the header. Therefore, the focus of temperature control of the horizontal header is to increase the temperature rise of the water supply section and keep the temperature of the water return section constant.

Because the buried depth has the greatest influence on the horizontal header, the first method to control the temperature of the water return section of the horizontal header is to increase the buried depth, then reduce the surface temperature, select a covering material with low thermal conductivity and reduce the flow in the pipe. At the same time, the method that best increases the temperature rise of the water supply section is to reduce the buried depth, increase the surface temperature, select a covering material with large thermal conductivity and increase the flow in the pipe, as shown in Figure 13.

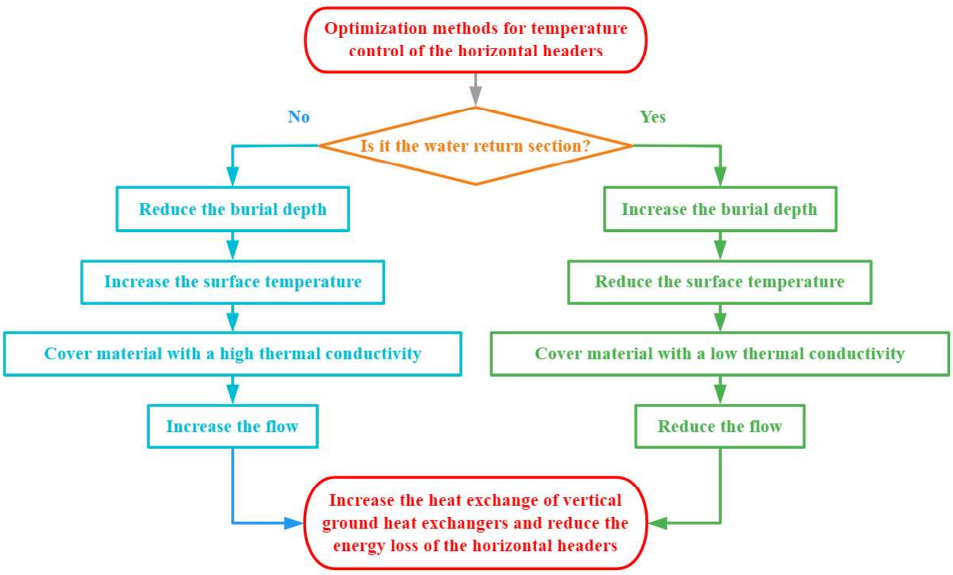

Fig. 13. Optimization methods for temperature control of the horizontal headers.

4.2. Recommendations for actual projects

Since the methods for controlling a constant temperature of the water return section of horizontal headers are opposite to the methods of increasing the temperature rise of the water supply section, comprehensive consideration should be taken to select appropriate temperature control methods. In actual projects, the surface temperature is uncontrollable, the flow of the water supply and return sections of horizontal headers is the same and the factors that can realize the independent control of the water supply and return sections are only the buried depth and the covering materials.

In actual projects, original soil and rock backfill are most commonly used, and there is no difference between the water supply and return sections. Therefore, within the working range of the unit, the buried depth of the water supply section of horizontal headers can be appropriately reduced to improve the end water temperature of the water supply section and enhance the heat exchange of vertical ground heat exchangers. At the same time, the buried depth of the water return section can be increased to keep the temperature in the pipe constant. When the water supply and return sections are buried at the same depth, in combination with economic analysis, pipes with low thermal conductivity or wrapped insulation materials can be used for the water return section to achieve the same effect.

In karst areas, the surface soil is very thin, and horizontal headers are mostly covered with excavated crushed rock. Due to the large thermal conductivity of the rock, the surface climate factors have a large impact on the headers. Therefore, it is necessary to consider increasing the buried depth of the return section of horizontal headers or taking thermal insulation measures to reduce the impact.

4.3. Research deficiencies and suggestions for extension

Many factors affect the heat transfer of horizontal headers. Due to the limitation of experimental conditions, this study only discusses the influence of four factors on horizontal headers: buried depth, buried pipe material, flow rate in the pipe and surface temperature. In the future, the influence of other factors can be discussed through experiments or numerical simulation, and the influence of a single factor on the temperature change of horizontal headers can also be studied in depth. In combination with the law of the temperature change of horizontal headers and the law of the change of a factor, the corresponding formula can be proposed to guide the actual project and reduce the energy loss of headers.

5. Conclusion

In this study, an orthogonal test is conducted on ground source heat pump horizontal headers. The temperature change of the horizontal header, the heat transfer of the header and the change of the heat exchange of the U-tube under the influence of the header temperature change are examined when the horizontal header is affected by four factors: buried depth, flow rate in the header, covering material and surface temperature. The influence factors are sorted by range analysis and the optimal scheme and the poor scheme are obtained. Finally, the optimization methods for horizontal header temperature control and the practical construction recommendations are put forward. The main conclusions are as follows:

(1) Regarding the horizontal header, the temperature rise of the water supply and return sections is 0.06 ℃ and 0.07 ℃, respectively under the most favourable working condition, and the heat transfer is 21.0 W and 24.5 W, respectively. The temperature rise of the water supply and return sections is 0.32 ℃ and 0.37 ℃, respectively under the most unfavourable working condition, and the heat transfer is 112.0 W and 129.5 W, respectively, which has a large impact.

(2) Under the most unfavourable conditions, the temperature rise of the water supply section is the largest, which increases the temperature difference between the U-tube and the surrounding rock and soil and promotes heat exchange. The heat exchange of the U-tube reaches 49.0 W, and the temperature difference between the inlet and outlet reaches 0.14 ℃. In contrast, under the most favourable conditions, the temperature rise of the water supply section is small, which is not conducive to the heat exchange of the U-tube. The heat exchange is 10.5 W and the temperature difference between the inlet and outlet is 0.03 ℃, which is a low value.

(3) Compared with all orthogonal test conditions, the inlet temperature of the U-tube under the initial condition is the lowest, which makes the heat exchange of the U-tube only 6.3 W, and the temperature difference between the inlet

and outlet is only 0.03 ℃, so the heat exchange effect is poor.

(4) The influence degree of each factor on horizontal headers is as follows: buried depth > surface temperature > covering material > flow in the pipe. The buried depth, surface temperature, covering material and flow rate in the pipe can be changed through different methods to achieve an optimal temperature control of the water supply and return sections, respectively.

(5) In the actual projects, the water supply section of horizontal headers can be buried above to increase the inlet water temperature of the U-tube, and the return section can be buried below to keep the temperature in the pipe constant. When the water supply and return sections are buried at the same depth, thermal insulation treatment can be carried out for the return section in combination with economic analysis, or pipes with low thermal conductivity can be used.

Declaration of Competing Interest

The authors declare that they have no known competing financial interests or personal relationships that could have appeared to influence the work reported in this paper.

Acknowledgements

This work was supported by the National Natural Science Foundation of China (NO. 52168013 and No. 5197041429), the Guizhou Provincial Science and Technology Project (No. ZK[2022]151, No. [2020]2004, No. [2018]5781-28 and No. [2019]1102) and the Guizhou University Science and Technology Project (No. [2019]66).

References

[1] WMO, State of the Global Climate 2021, Geneva, 2022. https://public.wmo.int/en.

[2] W. Zhou, P. Pei, R. Mao, H. Qian, Y. Hu, J. Zhang, Selection and techno-economic analysis of hybrid ground source heat pumps used in karst regions, Sci. Prog. 103 (2) (2020) 0036850420921682, https://doi.org/10.1177/0036850420921682.

[3] A. R. Puttige, S. Andersson, R. Östin, T. Olofsson, Modeling and optimization of hybrid ground source heat pump with district heating and cooling, Energy Build. 264 (2022) 112065, https://doi.org/10.1016/j.enbuild.2022.112065.

[4] C. Zhang, E. Nielsen, J. Fan, S. Furbo, Q. Li, Experimental investigation on a combined solar and ground source heat pump system for a single-family house: Energy flow analysis and performance assessment, Energy Build. 241 (2021) 110958, https://doi.org/10.1016/j.enbuild.2021.110958.

[5] Y. Jung, J. Oh, U. Han, H. Lee, A comprehensive review of thermal potential and heat utilization for water source heat pump systems, Energy Build. 266 (2022) 112124, https://doi.org/10.1016/j.enbuild.2022.112124.

[6] S. Maddah, M. Deymi-Dashtebayaz, O. Maddah, 4E analysis of thermal recovery potential of industrial wastewater in heat pumps: An invisible energy resource from the iranian casting industry sector, J. Clean Prod. 265 (2020) 121824, https://doi.org/10.1016/j.jclepro.2020.121824.

[7] U. Berardi, S. Jones, The efficiency and GHG emissions of air source heat pumps under future climate scenarios across Canada, Energy Build. 262 (2022) 112000, https://doi.org/10.1016/j.enbuild.2022.112000.

[8] S. Ran, W. Lyu, X. Li, W. Xu, B. Wang, A solar-air source heat pump with thermosiphon to efficiently utilize solar energy, J. Build. Eng. 31 (2020) 101330, https://doi.org/10.1016/j.jobe.2020.101330.

[9] Y. Zhang, Mass Transfer in Built Environment, China Architecture & Building Press, Beijing, 2006.

[10] A. Balbay, M. Esen, Experimental investigation of using ground source heat pump system for snow melting on pavements and bridge decks, Sci. Res. Essays 5 (24) (2010) 3955-3966.

[11] M. Esen, T. Yuksel, Experimental evaluation of using various renewable energy sources for heating a greenhouse, Energy Build. 65 (2013) 340-351, https://doi.org/10.1016/j.enbuild.2013.06.018.

[12] A. Widiatmojo, S. Chokchai, I. Takashima, Y. Uchida, K. Yasukawa, S. Chotpantarat, P. Charusiri, Ground-source heat pumps

with horizontal heat exchangers for space cooling in the hot tropical climate of Thailand, Energies 12 (7) (2019) 1274, https://doi.org/10.3390/en12071274.

[13] H. Esen, M. Inalli, M. Esen, Technoeconomic appraisal of a ground source heat pump system for a heating season in eastern Turkey, Energy Conv. Manag. 47 (9-10) (2006) 1281-1297, https://doi.org/10.1016/j.enconman.2005.06.024.

[14] H. Esen, M. Inalli, M. Esen, A techno-economic comparison of ground-coupled and air-coupled heat pump system for space cooling, Build. Environ. 42 (5) (2007) 1955-1965, https://doi.org/10.1016/j.buildenv.2006.04.007.

[15] X. Zhang, E. Wang, L. Liu, C. Qi, J. Zhen, Y. Meng, Analysis of the operation performance of a hybrid solar ground-source heat pump system, Energy Build. 268 (2022) 112218, https://doi.org/10.1016/j.enbuild.2022.112218.

[16] H. Esen, M. Inalli, A. Sengur, M. Esen, Modelling a ground-coupled heat pump system using adaptive neuro-fuzzy inference systems, Int. J. Refrig. 31 (1) (2008) 65–74, https://doi.org/10.1016/j.ijrefrig.2007.06.007.

[17] H. Esen, M. Inalli, A. Sengur, M. Esen, Predicting performance of a ground–source heat pump system using fuzzy weighted pre-processing-based ANFIS, Build. Environ. 43 (12) (2008) 2178–2187, https://doi.org/10.1016/j.buildenv.2008.01.002.

[18] H. Esen, M. Inalli, A. Sengur, M. Esen, Performance prediction of a ground–coupled heat pump system using artificial neural networks, Expert Syst. Appl. 35 (4) (2008) 1940–1948, https://doi.org/10.1016/j.eswa.2007.08.081.

[19] H. Esen, M. Inalli, A. Sengur, M. Esen, Modeling a ground-coupled heat pump system by a support vector machine, Renew. Energy 33 (8) (2008) 1814–1823, https://doi.org/10.1016/j.renene.2007.09.025.

[20] S. Dong, G. Liu, T. Zhan, Y. Yao, L. Ni, Performance study of cement-based grouts based on testing and thermal conductivity modeling for ground-source heat pumps, Energy Build. 272 (2022) 112351, https://doi.org/10.1016/j.enbuild.2022.112351.

[21] A. M. Bulmez, V. Ciofoaia, G. Năstase, G. Dragomir, A. I. Brezeanu, A. Şerban, An experimental work on the performance of a solar-assisted ground-coupled heat pump using a horizontal ground heat exchanger, Renew. Energy 183 (2022) 849-865, https://doi.org/10.1016/j.renene.2021.11.064.

[22] J. S. Jeon, S. R. Lee, M. J. Kim, S. Yoon, Suggestion of a scale factor to design spiral-coil-type horizontal ground heat exchangers, Energies 11 (10) (2018) 2736, https://doi.org/10.3390/en11102736.

[23] A. Pan, J. S. McCartney, L. Lu, T. You, A novel analytical multilayer cylindrical heat source model for vertical ground heat exchangers installed in layered ground, Energy 200 (2020) 117545, https://doi.org/10.1016/j.energy.2020.117545.

[24] S. Koohi-Fayegh, M. A. Rosen, Modeling of vertical ground heat exchangers, Int. J. Green Energy 18 (7) (2021) 755-774, https://doi.org/10.1080/15435075.2021.1880913.

[25] G. Hou, H. Taherian, Y. Song, W. Jiang, D. Chen, A systematic review on optimal analysis of horizontal heat exchangers in ground source heat pump systems, Renew. Sust. Energ. Rev. 154 (2022) 111830, https://doi.org/10.1016/j.rser.2021.111830.

[26] N. Kayaci, H. Demir, Numerical modelling of transient soil temperature distribution for horizontal ground heat exchanger of ground source heat pump, Geothermics 73 (2018) 33-47, https://doi.org/10.1016/j.geothermics.2018.01.009.

[27] R. Sangi, D. Müller, Dynamic modelling and simulation of a slinky-coil horizontal ground heat exchanger using Modelica, J. Build. Eng. 16 (2018) 159-168, https://doi.org/10.1016/j.jobe.2018.01.005.

[28] B. Xu, H. Zhang, Z. Chen, Study on heat transfer performance of geothermal pile-foundation heat exchanger with 3-U pipe configuration, Int. J. Heat Mass Transf. 147 (2020) 119020, https://doi.org/10.1016/j.ijheatmasstransfer.2019.119020.

[29] Q. Liao, Y. Fan, X. Zhu, J. Li, An Improved Thermal-Resistance-Capacitance Model for Vertical Single U-Tube Ground Heat Exchanger, J. Therm. Sci. Eng. Appl. 11 (1) (2019) 011016, https://doi.org/10.1115/1.4041437.

[30] X. Liu, M. He, Y. Wang, B. Zheng, C. Li, X. Zhu, Experimental study on heat transfer attenuation due to thermal deformation of horizontal GHEs, Geothermics 97 (2021) 102241, https://doi.org/10.1016/j.geothermics.2021.102241.

[31] C. Li, J. Mao, X. Peng, W. Mao, Z. Xing, B. Wang, Influence of ground surface boundary conditions on horizontal ground source heat pump systems, Appl. Therm. Eng. 152 (2019) 160-168, https://doi.org/10.1016/j.applthermaleng.2019.02.080.

[32] J. Chen, L. Xia, B. Li, D. Mmereki, Simulation and experimental analysis of optimal buried depth of the vertical U-tube ground heat exchanger for a ground-coupled heat pump system, Renew. Energy 73 (2015) 46-54, https://doi.org/10.1016/j.renene.2014.06.007.

[33] W. Zhou, P. Pei, D. Hao, C. Wang, A Numerical Study on the Performance of Ground Heat Exchanger Buried in Fractured Rock Bodies, Energies 13 (7) (2020) 1647, https://doi.org/10.3390/en13071647.

[34] L. Yang, B. Zhang, J. J. Klemes, J. Liu, M. Song, J. Wang, Effect of buried depth on thermal performance of a vertical U-tube underground heat exchanger, Open Phys. 19 (1) (2021) 327-330, https://doi.org/10.1515/phys-2021-0033.

[35] R. Wang, C. Yang, L. Ni, Y. Yao, Experimental study on heat transfer of soil with different moisture contents and seepage for ground source heat pump, Indoor Built Environ. 29 (9) (2020) 1238-1248, https://doi.org/10.1177/1420326x19894037.

[36] L. Pu, D. Qi, K. Li, H. Tan, Y. Li, Simulation study on the thermal performance of vertical U-tube heat exchangers for ground source heat pump system, Appl. Therm. Eng. 79 (2015) 202-213, https://doi.org/10.1016/j.applthermaleng.2014.12.068.

[37] C. Chen, W. Cai, D. Naumov, K. Tu, H. Zhou, Y. Zhang, H. Shao, Numerical investigation on the capacity and efficiency of a deep enhanced U-tube borehole heat exchanger system for building heating, Renew. Energy 169 (2021) 557-572, https://doi.org/10.1016/j.renene.2021.01.033.

[38] X. Song, M. Jiang, P. Qin, Numerical investigation of the backfilling material thermal conductivity impact on the heat transfer performance of the buried pipe heat exchanger, IOP Conf. Ser.: Earth Environ. Sci. 267 (4) (2019) 042010, https://doi.org/10.1088/1755-1315/267/4/042010.

[39] J. W. Lund, A. N. Toth, Direct utilization of geothermal energy 2020 worldwide review, Geothermics 90 (2021) 101915, https://doi.org/10.1016/j.geothermics.2020.101915.

[40] W. Li, X. Li, Y. Peng, Y. Wang, J. Tu, Experimental and numerical investigations on heat transfer in stratified subsurface materials, Appl. Therm. Eng. 135 (2018) 228-237, https://doi.org/10.1016/j.applthermaleng.2018.02.037.

[41] E. Marin, A. Calderon, O. Delgado-Vasallo, Similarity theory and dimensionless numbers in heat transfer, Eur. J. Phys. 30 (3) (2009) 439-445, https://doi.org/10.1088/0143-0807/30/3/001.

[42] W. Tao, Heat Transfer, fifth ed., Higher Education Press, Beijing, 2019.

[43] W. Li, X. Li, R. Du, Y. Wang, J. Tu, Experimental investigations of the heat load effect on heat transfer of ground heat exchangers in a layered subsurface, Geothermics 77 (2019) 75-82, https://doi.org/10.1016/j.geothermics.2018.08.011.

[44] X. Yang, G. Liu, Y. Li, S. Gao, Structural optimization of reciprocating seal with magnetic fluid based on orthogonal test design, J. Magn. 26 (2) (2021) 229-237, https://doi.org/10.4283/JMAG.2021.26.2.229.

[45] M. Jin, M. R. Islam, L. Li, M. H. Rahman, Contact stress and bending stress calculation model of spur face gear drive based on orthogonal test, Microsyst. Technol. 26 (4) (2020) 1055-1065, https://doi.org/10.1007/s00542-019-04630-w.

[46] M. Zheng, Y. Wang, H. Teng, A novel method based on probability theory for simultaneous optimization of multi-object orthogonal test design in material engineering, Kov. Mater.-Met. Mater. 60 (2022) 45-53, https://doi.org/10.31577/km.2022.1.45.

[47] Y. Luo, G. Xu, T. Yan, Performance evaluation and optimization design of deep ground source heat pump with non-uniform internal insulation based on analytical solutions, Energy Build. 229 (2020) 110495, https://doi.org/10.1016/j.enbuild.2020.110495.

[48] S. Su, R. Yang, L. Liu, C. Zhou, L. Shi, Study on the Influential Factors of Heat Transfer of Ground Heat Exchanger with Orthogonal Test, IOP Conf. Ser.: Earth Environ. Sci. 81 (2017) 012166, https://doi.org/10.1088/1755-1315/81/1/012166.

[49] C. Li, Y. Guan, Y. Feng, C. Jiang, S. Zhen, X. Su, Comparison of influencing factors and level optimization for heating through deep-buried pipe based on Taguchi method, Geothermics 91 (2021) 102045, https://doi.org/10.1016/j.geothermics.2021.102045.

[50] S. Gharibi, E. Mortezazadeh, S. J. Hashemi Aghcheh Bodi, A. Vatani, Feasibility study of geothermal heat extraction from abandoned oil wells using a U-tube heat exchanger, Energy 153 (2018) 554-567, https://doi.org/10.1016/j.energy.2018.04.003.

[51] A. Jahanbin, G. Semprini, A. Natale Impiombato, C. Biserni, E. Rossi di Schio, Effects of the Circuit Arrangement on the Thermal Performance of Double U-Tube Ground Heat Exchangers, Energies 13 (12) (2020) 3275, https://doi.org/10.3390/en13123275.

[52] X. Yang, G. Liu, Y. Li, S. Gao, Structural optimization of reciprocating seal with magnetic fluid based on orthogonal test design, J. Magn. 26 (2) (2021) 229-237, https://doi.org/10.4283/JMAG.2021.26.2.229.